8 Nuclear deformations and the unified model

The first attempt to improve the single-particle shell model (SPSM) was to consider nuclei with just two or three particles outside a closed shell and to remove the degeneracy, not by the pairing force of the SPSM, but by a more general residual interaction. The coupling of the individual spin and orbital angular momenta was treated by the methods developed by Racah for atomic spectroscopy in which either the *jj* or the *LS* (Russell–Saunders) scheme may be used. Observed nuclear spectra may require a coupling scheme intermediate between the two extremes. When both types of nucleon are involved use is generally made of the assumption of charge independence and total isobaric spin T then provides an additional quantum number. The model that thus develops from the extreme single-particle model is known as the *independent-particle model* (IPM); it regards the first few nucleons outside a closed shell as essentially *equivalent.*

IPM calculations often improve the prediction of magnetic moments, but are unable to explain the enhanced electric quadrupole moments of the rare-earth nuclei, for which a stronger cooperative effect is required. This effect must involve the nucleons not only of unfilled shells but also of the closed shells that have so far been disregarded except for their presumed role in providing the central potential with respect to which single-particle motion may be defined. The recognition of the interaction between the loose or 'valence' nucleons and the nucleons of the core in producing coherent collective nuclear motion was an achievement for which Rainwater, A. Bohr and Mottelson were awarded the Nobel Prize of 1975. Their work, dating from the early 1950s, is essentially the theory of nuclear deformations.

A deformed nucleus will generate a deformed potential well, in which neither the total nor the orbital angular momentum of a single particle is a good quantum number because of lack of spherical symmetry. Shell-model calculations should be based on this potential. The way to do this was shown by Nilsson and the model resulting, which generalizes the SPSM, is known as the

unified model. In this chapter some of the properties of deformed nuclei will be examined and related to this model.

8.1 Early empirical evidence for collective motion and for nuclear deformation

8.1.1 The compound nucleus

The nature of the nucleon motion within a nucleus determines the general character of its excitation energies. If it is possible to describe the nucleus as a mechanical system with a small number of degrees of freedom, the energy eigenvalues will be well separated, and this is essentially the prediction of the SPSM. If, however, many degrees of freedom exist, as might be expected if there is strong coupling between individual nucleons, then the number of states per unit energy range will increase considerably.

Information on nuclear level densities at about 8 MeV excitation became available in 1935 as a result of experiments with neutrons of near-thermal energies. For such particles the (n, γ) capture reaction, e.g.

$$^{107}\mathrm{Ag} + \mathrm{n} \rightarrow {}^{108}\mathrm{Ag} + \gamma \tag{8.1}$$

is easily observable, by detection of the radioactivity of the product nucleus, e.g.

$$^{108}\mathrm{Ag} \rightarrow {}^{108}\mathrm{Cd} + \beta^- + \bar{\nu} \tag{8.2}$$

or by a transmission experiment, and the variation of the cross-section with energy can be studied. According to the SPSM the neutron would move only briefly in the potential well provided by the target nucleus and would have a high probability of emerging (Fig. 8.1*a*); resonance would be observed when the incident particle created a system with an energy near one of the levels of the potential well, but the spacing of these would be $\approx \hbar^2/2MR^2$, i.e. about 1 MeV for $A \approx 100$. Also, the width would be large ($\approx$1 MeV) because of the brief time of association ($\approx 10^{-21}$ s) of the neutron with the well. Variations of capture probability with energy in the thermal range are not likely to be produced by these resonances.

This picture is in sharp disagreement with observation at several points. Although the single-particle resonances are seen as broad structural features in scattering cross-sections as a function of energy for neutrons of a few MeV energy, near-thermal neutrons show small scattering and large absorption for many nuclei. In particular, the work of Moon and Tillman and of Amaldi and Fermi, using reactions such as (8.1) and (8.2), established not only the existence of thermal neutrons in systems in which slowing down

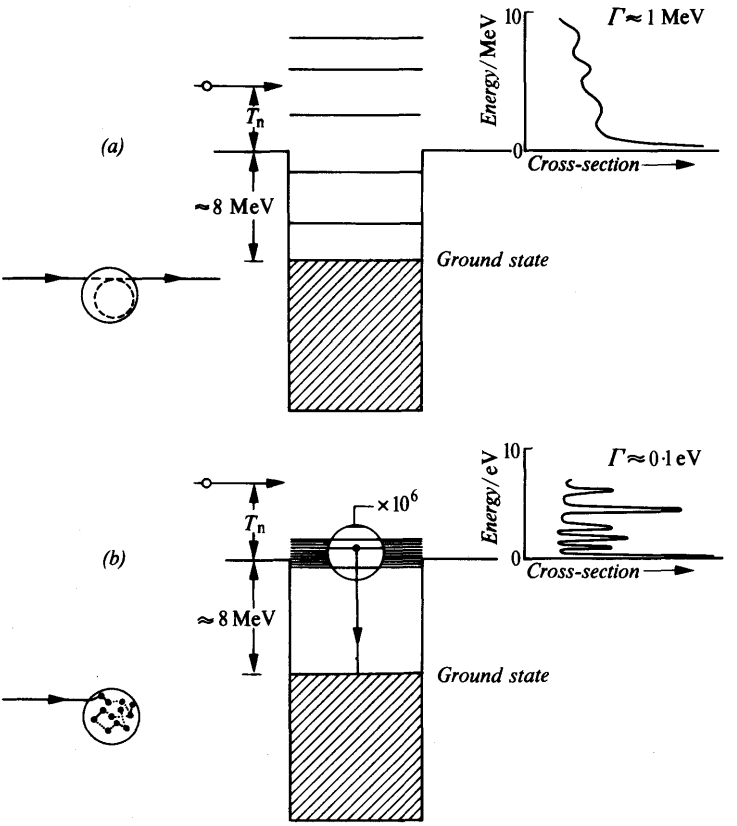

Fig. 8.1 Interaction of a neutron with a nucleus. The levels shown represent states of excitation of the system (neutron + nucleus); a neutron of zero laboratory energy T_n produces an excitation of about 8 MeV: (*a*) Potential-well model. (*b*) Compound-nucleus model. Note the different energy scales.

could take place, but also anomalies in cross-section for near-thermal energies that had to be interpreted as due to *narrow, relatively long-lived* resonant states (Fig. 8.1*b*).

In order to explain these observations, Niels Bohr in 1936 introduced the concept of the *compound nucleus*, which is a many-body system formed by the amalgamation of the incident particle with the target nucleus, e.g. reaction (8.1) proceeds in two stages:

$$\left.\begin{aligned} {}^{107}\mathrm{Ag} + \mathrm{n} &\rightarrow {}^{108}\mathrm{Ag}^* \\ {}^{108}\mathrm{Ag}^* &\rightarrow \text{final state} \end{aligned}\right\} \tag{8.3}$$

where $^{108}Ag^*$ represents a ^{108}Ag nucleus plus the energy brought in by the incident neutron, which is the separation energy S_n plus a

very small kinetic energy ε. In such a system the incident particle has a short mean free path and shares the total energy $S_n+\varepsilon$ with many of the internal degrees of freedom of the compound nucleus, so that it cannot be re-emitted until, as a result of further exchanges, sufficient energy ($>S_n$) is again concentrated on this or a similar particle. If the incident particle is a slow neutron ($\varepsilon \approx 0$) this may be a very long time, several orders of magnitude greater than the time that a fast particle takes to cross the nucleus, and this time ($\approx 10^{-14}$ s) may be long enough to permit the electromagnetic coupling to generate the emission of a photon so that (8.3) is completed by the process

$$^{108}\mathrm{Ag}^* \rightarrow {}^{108}\mathrm{Ag}+\gamma \tag{8.4}$$

as shown in Fig. 8.1*b*.

The clear experimental evidence for the compound nucleus in slow-neutron capture reactions indicates the closely coupled nature of nuclear motion, and consequently the possibility of collective modes. In the early theories of N. Bohr and Kalckar, the dynamical situation was likened to that of a classical liquid drop and this concept was fruitful in the evolution of the semi-empirical mass formula (Sect. 6.3) and in the theory of fission (Sect. 11.7.2). It is now more useful, in the light of present knowledge of nuclear densities and Fermi momenta, to speak of a Fermi gas rather than a Fermi liquid, but the feature of collective motion applies equally to each. The application of statistical methods to the compound nucleus level system at high excitations has also shown agreement with many features of nuclear reactions and confirms the concept of correlated motion.

8.1.2 Radius anomalies

Electron scattering experiments (Sect. 6.2) determine the mean-square radius of the nuclear charge distribution and show that it varies with mass number in accordance with the formula

$$\langle r^2 \rangle \propto A^{2/3} \tag{8.5}$$

for the natural sequence of nuclei in which roughly equal numbers of protons and neutrons are added in passing from one nucleus to another. If only neutrons are added, the change in $\langle r^2 \rangle$ should be given, according to (8.5), by

$$\delta\langle r^2 \rangle / \langle r^2 \rangle = 2\delta A/3A \tag{8.6}$$

Such a change in nuclear dimensions will cause an *isotope shift* (volume or field effect) in the lines of optical, X-ray and muonic atom spectra, additional to the shift expected from the mass change. Optical spectroscopic observations available in 1958 for pairs of

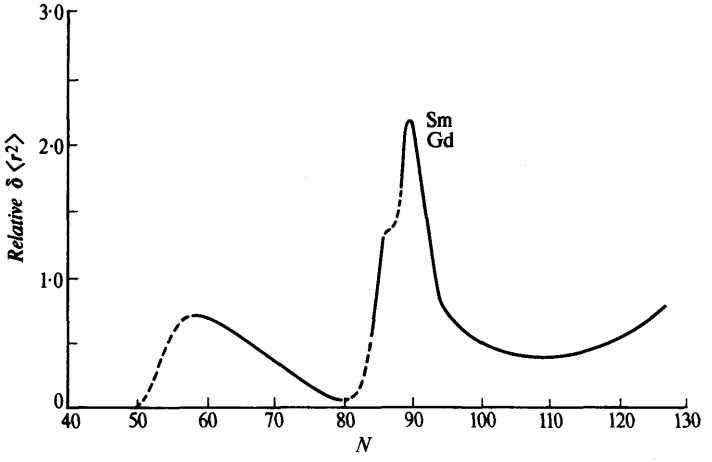

Fig. 8.2 Relative $\delta\langle r^2\rangle$ from isotope shifts as a function of neutron number N. The line represents the trend of observed shifts (Ref. 6.2).

even–even nuclei differing in neutron number by two (N and $N-2$) indicated changes of $\langle r^2\rangle$, relative to that predicted by equation (8.6), as shown in Fig. 8.2. The jump in $\delta\langle r^2\rangle$ between $N=88$ and $N=90$ is entirely unconnected with any features of the SPSM and represents the onset of a deviation of the nuclear shape from spherical symmetry. Later and more comprehensive experimental evidence on deformation shows that it vanishes for closed-shell nuclei.

8.1.3 Origin of nuclear deformation

The original proposal by Rainwater, elaborated and developed by Bohr and Mottelson, was based on the liquid-drop model of the nucleus, as already used in setting up the semi-empirical mass formula (Sect. 6.3). This formula indicates that since for a given volume a spherical shape has the minimum surface area, deformed nuclei should have an energy increasing with the square of a suitable parameter, such as the change of major axis, representing the deformation. This situation is represented in Fig. 8.3, curve (*a*).

If the motion of the individual nucleons is considered, the spherical equilibrium shape for nuclei with a few nucleons outside closed shells or subshells may be ascribed to the pairing force. The collective motion in this case is a vibration about the spherical shape. As the number of 'valence' nucleons increases, however, distorting forces due to the quadrupole component of the internucleon force may become important. The frequency of the collective vibration

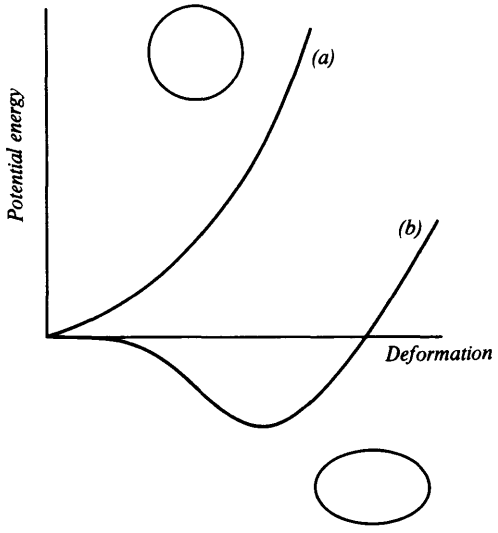

Fig. 8.3 Potential energy of a nucleus as a function of deformation. (*a*) Spherical shape. (*b*) Deformed shape.

diminishes and finally the spherical shape becomes unstable and the nucleus acquires a *permanent* deformation. The origin of this may be understood by considering the actual orbital motion of the nucleons; if a deformation of the core occurs the outer nucleons move to 'orbits' of larger radius and if the angular momentum stays constant, the kinetic energy *decreases* as the radius parameter increases. Equilibrium is reached at the stable deformation (Fig. 8.3, curve (*b*)).

A few nucleons of one kind and of given l outside a closed shell, with the nucleons of the other kind paired off, would tend to occupy equatorial orbits of high m-values. Interaction of these nucleons with the core would produce an equatorial bulge, which corresponds with a negative quadrupole moment (Fig. 8.4*a*). If, however, there are *holes* in the closed shell the opposite behaviour is favoured and a positive quadrupole moment develops when there are sufficient holes (Fig. 8.4*c*). At the closed-shell nucleon number the moment is zero (Fig. 8.4*b*). This variation of quadrupole moment with nucleon number is also expected according to the single-particle model (Table 7.1), but the present picture shows how the moments may be enhanced, and indeed very much enhanced if a stable deformation exists.

If there is such a deformation, then as pointed out by A. Bohr vibrational and rotational motion of the deformed nucleus may co-exist with the intrinsic motion of the individual nucleons that

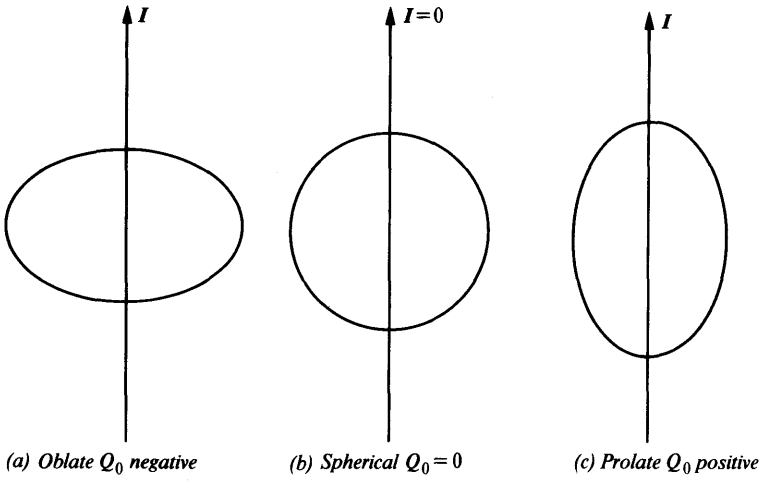

Fig. 8.4 Intrinsic quadrupole moments Q_0.

creates the deformed shape. It is necessary for a simple development of the theory of this coupled collective motion that the single-particle energies associated with the shell-model nucleon states should be large compared with the vibrational and rotational energies so that the period of the collective motions is relatively long and it is sensible, for instance, to define a moment of inertia. The collective excitations then provide a fine structure in the overall pattern of intrinsic, e.g. single-particle, states. At the same time the deformation of the nucleus has a profound effect not only on the static electromagnetic moments but also on radiative transition rates, which are often enhanced above single-particle values.

The simplest type of deformation is ellipsoidal, with an axis of symmetry Oz', as shown in Fig. 8.5. The axis Oz' is fixed in the nucleus but may orient with respect to a space-fixed axis Oz. The magnitude of this type of deformation may be specified by a parameter δ given by

$$\delta = \Delta R / R_0 \tag{8.7}$$

where R_0 is the average nuclear radius and ΔR is the difference between the major and minor semi-axes of the ellipse. Alternatively, the angular shape in a plane containing Oz' may be defined by the expression

$$R(\theta) = R_0[1 + \beta Y_2^0(\theta, \phi)] \tag{8.8}$$

where θ is the angle with Oz', and $\beta = 1{\cdot}06\delta$, using the normalized form of Y_2^0 (Appendix 1).

The deformation parameter δ (or β) is typically 0·2–0·3 and is obtained from measurements of electromagnetic transition rates (Sect. 8.5) and from the pattern of rotational states (Sect. 8.2) as well as from isotope shifts. All evidence confirms that the jump found between $N = 88$ and $N = 90$ in Fig. 8.2 represents a transition between the vibrational and rotational type of collective motion.

8.2 Rotational states

8.2.1 Coupling of angular momenta

The coupling of angular momenta in a deformed nucleus resembles that in molecules and is shown in Fig. 8.5. It is assumed, in the circumstances outlined in Section 8.1.3, that the nuclear wave-function is a product of an intrinsic function and a rotational function, and it is the latter with which we are mainly concerned in this section. The intrinsic motion, with resultant angular momentum

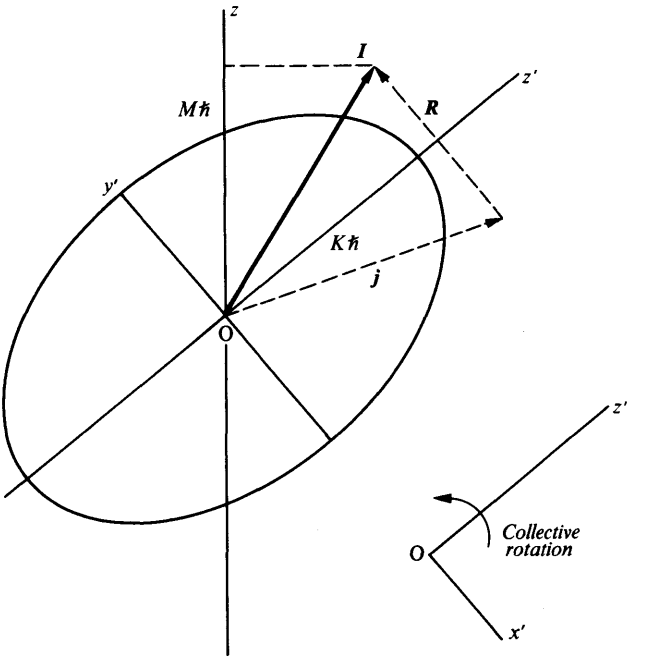

Fig. 8.5 Cross-section of axially symmetric deformed nucleus, showing body-fixed axis Oz′ and space-fixed axis Oz. The total angular momentum vector $\boldsymbol{I}$ is indicated; $M\hbar$ is the resolved part of $\boldsymbol{I}$ along Oz and $K\hbar$ the resolved part along Oz′. $\boldsymbol{R}$ is the vector representing collective rotation, which adds vectorially to the intrinsic angular momentum $\boldsymbol{j}$ to form $\boldsymbol{I}$.

$\boldsymbol{j}$, is related to the body-fixed axis Oz', but in the non-spherical field $\boldsymbol{j}$ is not a constant of the motion. Rather, it couples with any collective rotational angular momentum $\boldsymbol{R}$ to give the total resultant angular momentum $\boldsymbol{I}$ of the nucleus, which *is* a constant of the motion, as is its component $M\hbar$ along the space-fixed axis Oz.

Because Oz' is an axis of symmetry the orientation of the body-fixed axes cannot be uniquely specified and this means (Ref. 8.1) that there is no collective rotation about Oz'. This is so for the case of diatomic molecules and also for spherical nuclei, which do not show rotational bands of the type discussed in this section. Consequently, $\boldsymbol{R}$ is perpendicular to the symmetry axis. Moreover, since the system is invariant to rotations about Oz', the component $K\hbar$ of the angular momentum $\boldsymbol{I}$ is also a constant of the motion. Figure 8.5 shows that $K\hbar$ is also the component of the intrinsic angular momentum along Oz'. Together the three observables $\boldsymbol{I}^2$, $M\hbar$ and $K\hbar$ completely specify the state of motion.

From Fig. 8.5, the rotational angular momentum is given by $\boldsymbol{R}=\boldsymbol{I}-\boldsymbol{j}$. If however averaging of the intrinsic motion is assumed it is possible to write

$$\boldsymbol{R}^2=\boldsymbol{I}^2+\boldsymbol{j}^2-2\boldsymbol{I}.\boldsymbol{j}=\boldsymbol{I}^2+\boldsymbol{j}^2-2K^2\hbar^2 \tag{8.9}$$

except in the case of $K=\frac{1}{2}$, and this expression will be used in the following discussion.

8.2.2 *Energy levels*

The energy of collective rotation may be written in the classical form

$$E_R=\tfrac{1}{2}\mathcal{I}\omega^2 \tag{8.10}$$

where ω is the angular velocity about the axis of rotation, which is perpendicular to the symmetry axis, as shown in Fig. 8.5, and $\mathcal{I}$ is a moment of inertia. If the rotational angular momentum $\mathcal{I}\omega=|\boldsymbol{R}|$ is inserted in (8.10) we find, except in the case of $K=\frac{1}{2}$,

$$E_R=(\hbar^2/2\mathcal{I})[I(I+1)+j(j+1)-2K^2] \tag{8.11}$$

using the eigenvalues for $\boldsymbol{I}^2$ and $\boldsymbol{j}^2$, and for the rotational energies referred to the ground state

$$E_{\text{rot}}=E_I-E_{\text{g}}=(\hbar^2/2\mathcal{I})[I(I+1)-I_{\text{g}}(I_{\text{g}}+1)] \tag{8.12}$$

The value of K ($\leqslant I_{\text{g}}$) arising from the intrinsic motion thus determines a *rotational band* of levels, whose extra energies are added to that of the intrinsic motion, as in the case of molecular rotational states.

For *even–even nuclei in their ground state* the individual particles are paired and fall alternatively into states of opposite K, so that the

resultant K-value is zero with even parity. Because of the symmetry about a plane perpendicular to Oz', only even I-values occur (as in the case of the homonuclear diatomic molecule obeying Bose statistics), and the spin-parity values for the rotational band are

$$K=0 \qquad I=0^+, 2^+, 4^+, 6^+, \ldots \tag{8.13}$$

The total angular momentum arises solely from the collective rotation.

Clearly defined rotational bands are found in even–even nuclei with N and Z values lying within the ranges shown in Fig. 8.6*a*, and a well-known rotational band is shown in Fig. 8.6*b*. The levels of the band may be excited electromagnetically (Coulomb excitation, Sect. 9.4.2) and they decay mainly by the emission of electric quadrupole radiation (Sect. 9.2). The ratios of excitation energies in rotational band are (from (8.12) with $K=I_g=0$) $E_4/E_2=10/3$, $E_6/E_2=7$, and $E_8/E_2=12$, independently of the moment of inertia, providing that this is independent of rotational frequency.

The actual value of the effective moment of inertia $\mathcal{I}$ is model-dependent. If the nucleus behaved as a rigid object of mass AM where A is the number of component nucleons of mass M then the classical rigid-body value would be

$$\mathcal{I}_{\text{rig}}=(\tfrac{2}{5})AMR^2 \tag{8.14}$$

where R is a mean radius and would be found by analysis of the spacings in the rotational band. It can be shown that this rigid-body value is also obtained in the shell model with wholly independent particle motion. Pairing forces, however, inhibit this independence and the motion then exhibits a lower moment of inertia; observed values are, in fact, smaller than the rigid value by a factor of 2–3 for low I-values.

The moment of inertia is not always constant, as would be expected for a rigid body, throughout a rotational band. From an experimental spectrum such as that shown in Fig. 8.6*b*, but more particularly for the even–even rare-earth nuclei, the moment of inertia is given by

$$2\mathcal{I}/\hbar^2=(4I-2)/(E_I-E_{I-2}) \tag{8.15}$$

Also, the angular velocity of rotation for the state I is obtained with a small approximation for $I\gg 1$ as

$$(\hbar\omega)^2=\tfrac{1}{4}(E_I-E_{I-2})^2 \tag{8.16}$$

where E_I and E_{I-2} are the energies E_R of equation (8.11) with $K=0$. A plot of $2\mathcal{I}/\hbar^2$ against $(\hbar\omega)^2$ is given in Fig. 8.7. It shows firstly an increase of $\mathcal{I}$ with ω up to spin values ≈ 15 and this can be understood in terms of a centrifugal stretching as ω increases (variable moment of inertia). For some even–even nuclei there then

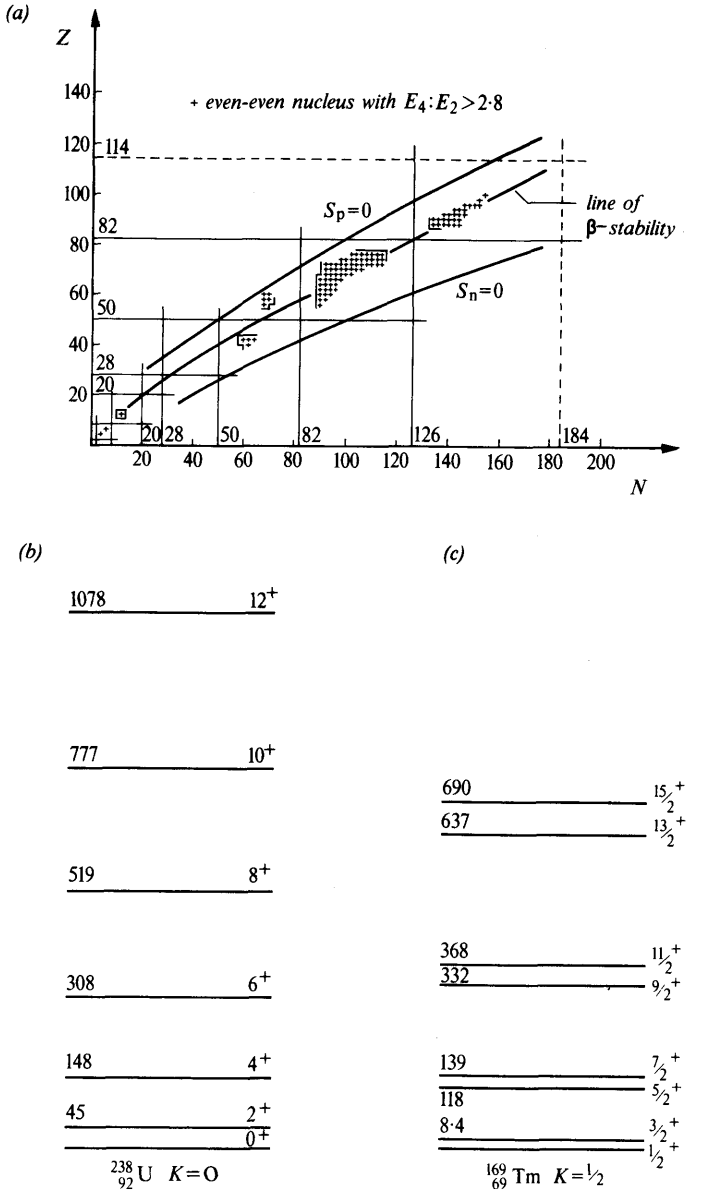

Fig. 8.6 (*a*) Regions of deformed even–even nuclei (+). The lines $S_p=0$, $S_n=0$ give the stability limits for proton and neutron emission (Ref. 8.1). (*b*) Ground-state rotational band in ^{238}U. (*c*) Ground-state rotational band in ^{169}Tm. Energies in keV and spin-parities I^π are shown.

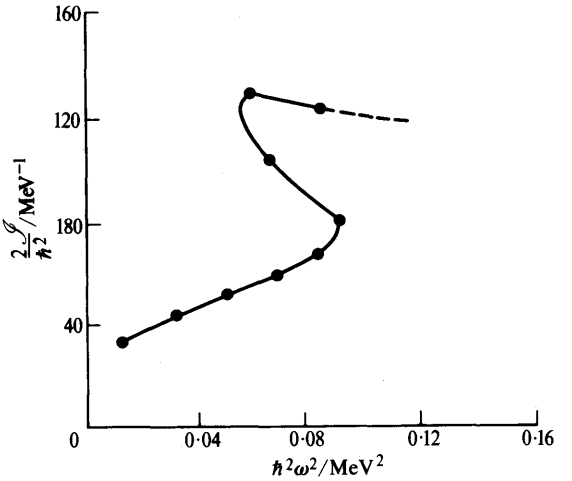

Fig. 8.7 Collective moment of inertia as a function of angular velocity squared for $^{158}_{68}$Er (Grosse, E. *et al.*, *Phys. Rev. Letters* **31,** 840, 1973).

ensues the striking phenomenon of *back-bending*, in which there is a sharp increase of $\mathcal{I}$ towards the rigid value. One explanation of this effect is that it is a disappearance of the pairing correlation due to the action of Coriolis forces; the nucleus then undergoes a phase transition from a superfluid state to a state of independent-particle motion. Alternatively, just one pair of neutrons, for instance, is broken, providing a large angular momentum which may couple with the collective rotation to produce a new band. Such effects will depend on the actual value of the pairing energy and will not be seen for all nuclei. It may be noted at this point that, in general, the rotational states of an even–even nucleus lie *within* the energy gap predicted in the spectrum of intrinsic states (Sect. 6.4.3).

In even–even nuclei with an excitation from the intrinsic motion, and in *odd-A nuclei*, K is finite; in the latter case the last odd particle at least contributes a component of angular momentum along the symmetry axis Oz'. The energy levels have spin values given by

$$K \neq 0 \qquad I = K, K+1, K+2, \ldots \tag{8.17}$$

and these are integral for A even and half-integral for A odd. The parity is that of the intrinsic motion. The states with $I_{z'} = \pm K$ have equal energy, and for $K = \frac{1}{2}$ the Coriolis forces in the rotating system connect these states and give rise to an extra term in the rotational energy. For a state of spin I this is found to be, apart from a constant term,

$$E_R = (\hbar^2/2\mathcal{I})[I(I+1) + a(-1)^{I+1/2}(I+\tfrac{1}{2})] \tag{8.18}$$

The decoupling term $a(I+\frac{1}{2})$ has opposite sign for the successive levels of a $K=\frac{1}{2}$ band and the level spacing is considerably modified from the $I(I+1)$ interval found for $K=0$ (Fig. 8.6*c*).

For $K>\frac{1}{2}$ the additional term is much smaller and the excitation energies with respect to the ground state $I_g=K$ are well approximated by equation (8.12).

Although the rotational bands so far discussed have a relatively simple structure, the nuclear spectrum contains many more states deriving from vibrational modes (Sect. 8.4) and from special couplings. The lowest level of given I, however, has a special significance because of its intimate connection with the joint effects of collective motion and pair correlation; it is referred to as the *yrast* level.

8.3 Single-particle motion in a deformed potential

For nuclei which have an ellipsoidal deformation, the nuclear radius is given by equation (8.8) and the nuclear potential would be expected to follow this form, e.g.

$$V(r,\theta)=V_0(r)+V_2(r)Y_2^0(\theta,\phi) \tag{8.19}$$

In this expression the first term may be identified with the customary Saxon–Woods form of a spherical potential (Sect. 7.2.4).

For *small deformations* it will be permissible to use the single-particle quantum numbers n, l, j appropriate to a spherical potential, remembering that for axial symmetry the projection Ω of the total angular momentum $\boldsymbol{j}$ along the symmetry axis is a constant of the motion. The energies may then be obtained by treating the second term of (8.19) as a perturbation, and are found to be (Ref. 8.1)

$$\varepsilon(nlj\Omega)=\varepsilon_0(nlj)-\frac{3\Omega^2-j(j+1)}{4j(j+1)}\langle V_2(r)\rangle_{nlj} \tag{8.20}$$

with $\Omega=\pm\frac{1}{2},\pm\frac{3}{2},\ldots,\pm j$. There is degeneracy with respect to Ω since positive and negative values have the same energy. Each undeformed shell-model level then splits into $\frac{1}{2}(2j+1)$ distinct states labelled by Ω, which is also equal to K as used in Section 8.2.

For rather *large deformations*, more characteristic of the collective model, neither j nor l is a good quantum number. An approximate description of the single-particle motion is obtained by considering an anisotropic harmonic oscillator potential

$$V=\tfrac{1}{2}M[\omega_3^2x_3^2+\omega_\perp^2(x_1^2+x_2^2)] \tag{8.21}$$

where x_1, x_2 and x_3 are Cartesian coordinates and ω_3 and $\omega_\perp$ are the axial and transverse oscillation frequencies. The energies are then

$$\varepsilon(n_3n_\perp)=(n_3+\tfrac{1}{2})\hbar\omega_3+(n_\perp+1)\hbar\omega_\perp \tag{8.22}$$

where $n_\perp = n_1 + n_2$ is the oscillator number for the motion perpendicular to the symmetry axis. There is a degeneracy associated with $n_\perp$ but it may be labelled by the component Λ of the orbital momentum along the symmetry axis. Further degeneracy arises because of the possible positive and negative alignment of the intrinsic spin Σ $(=\frac{1}{2})$ of the nucleon along the symmetry axis. Together with Λ this produces the component $\Omega = \Lambda \pm \Sigma$ already discussed.

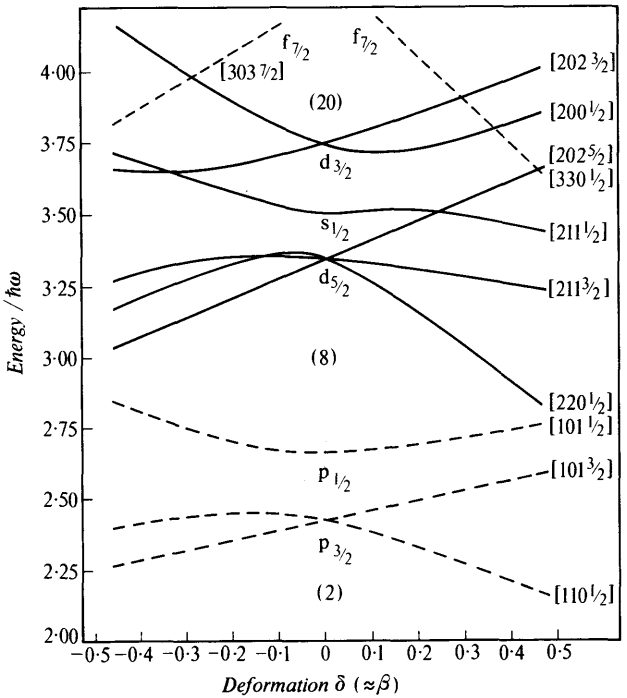

Fig. 8.8 Spectrum of single-particle orbits in spheroidal potential ($N, Z < 20$) (Ref. 8.1). The level energies are in units of the oscillator spacing (eqn (7.3)) and are plotted as a function of the deformation parameter δ ($\approx\beta$) (eqn (8.7)). The individual labels are the asymptotic quantum numbers (Sect. 8.3).

Couplings exist which remove these degeneracies and it is then useful to label the resulting states by the numbers N $(=n_3+n_\perp)$, n_3, Λ, Ω. They are known as *asymptotic quantum numbers* since they really apply in the limit of large deformations when the (n, l, j, Ω) scheme is invalid. The one-particle spectra obtained by use of an oscillator potential of the form (8.21) with an averaged frequency ω together with terms designed to remove the degeneracies, are shown for N and $Z < 20$ in Fig. 8.8.

8.4 Vibrational states

8.4.1 Vibrational quanta (phonons)

In Section 8.1.3 it was noted that nuclei with a few nucleons outside closed shells, and the closed-shell nuclei themselves, have a spherical equilibrium shape. The simplest collective motion of such a system is a simple harmonic vibration of the surface about equilibrium. The corresponding energies give rise to levels in the nuclear spectrum which, as in the case of the corresponding levels in molecular physics, have a somewhat greater spacing than the levels of a rotational band.

Nuclear surface vibrations may be discussed classically using the model of an incompressible liquid drop. The instantaneous form of the surface may be described generally by an expansion in terms of spherical harmonics

$$R(\theta, \phi) = R_0\left(1 + \sum_{\lambda,\mu} \alpha_{\lambda\mu}(t) Y_\lambda^\mu(\theta, \phi)\right) \tag{8.23}$$

of which equation (8.8) is a particular case, with $\lambda = 2$, $\mu = 0$. The vibrations about equilibrium are governed by a potential-energy curve of the form shown in Fig. 8.3*a* and the total energy for a given λ may be written in terms of a force parameter C and a mass parameter D

$$E = \tfrac{1}{2}C\alpha^2 + \tfrac{1}{2}D\dot{\alpha}^2 \tag{8.24}$$

with an oscillation frequency given by

$$\omega_\lambda = \sqrt{C/D} \tag{8.25}$$

Solution of the equation of motion shows that a surface vibration may be described classically in terms of waves that travel round the z-axis $\theta = 0$. These waves carry angular momentum.

If the oscillations are quantized (compare the treatment of the single particle in an oscillator potential, Sect. 1.4.2) the energies have the values

$$E_n = \hbar\omega_\lambda \sum_\mu (\tfrac{1}{2} + n_\mu) = \hbar\omega_\lambda\left(\frac{2\lambda + 1}{2} + n\right) \tag{8.26}$$

where λ is, of course, integral, $|\mu| \leqslant \lambda$ and n_μ is the number of oscillator quanta in a state (λ, μ). The oscillator number $n = \sum_\mu n_\mu = 0, 1, 2, \ldots$ is the total number of such quanta. The excitation energy is thus determined by the number of quanta, or *phonons* present in the state. Phonons may be regarded as particles each carrying an angular momentum $\lambda\hbar$, parity $(-1)^\lambda$ and energy $\hbar\omega_\lambda$; like photons

they obey Bose–Einstein statistics. The spin values of vibrational states follow directly from their phonon content.

The inertial parameters C and D are functions of λ and may be estimated by classical calculations which show that ω_3 (octupole phonon) $\approx 2\omega_2$ (quadrupole phonon). The phonon energies indicated by experiment (cf. Fig. 8.11) are $\approx 0{\cdot}5$ MeV and must be distinguished from the very much larger energies (≈ 10 MeV) associated with the single-particle oscillator spacing of the shell model. In terms of that model, the surface waves correspond with excitations not requiring any change of the single-particle oscillator number N.

8.4.2 *Energy levels (spherical equilibrium)*

In the following sequence, $\lambda = 0$ and $\lambda = 1$ excitations are included for completeness, although they are high-energy modes and are not appropriately described as surface vibrations.

(i) $\lambda = 0$ (Fig. 8.9*a*). This is a wholly radial oscillation and is not possible for an incompressible fluid. Nuclear matter is not incompressible, but no monopole state of this sort ('breathing mode') has

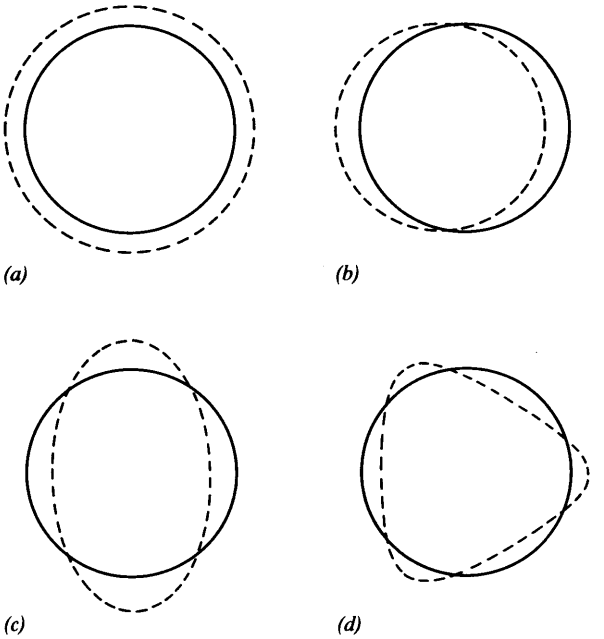

Fig. 8.9 Modes of nuclear vibration about a spherical equilibrium state (solid line). The dotted line shows one extreme excursion of the nuclear surface. (*a*) $\lambda = 0$. (*b*) $\lambda = 1$, relevant to opposite motions of neutron and proton fluids. (*c*) $\lambda = 2$. (*d*) $\lambda = 3$.

been identified with certainty and such 0^+ states if they exist probably lie high in the nuclear spectrum (Fig. 8.16*b*). The 0^+ states known at fairly low excitation in even–even nuclei, such as ^{16}O, ^{72}Ge and ^{90}Zr can be given a shell-model interpretation.

(ii) $\lambda = 1$ (Fig. 8.9*b*). This is a dipole deformation which corresponds with a displacement of the centre of mass and can only be produced by external forces. If such a displacement is imposed on a nucleus in which the neutrons and protons behave as a homogeneous fluid, and always move in phase, the centre of charge always coincides with the centre of mass and no electric dipole moment can arise. If, however, the neutrons and protons behave as separate fluids and move in antiphase, the centres of charge and mass separate and a dipole moment develops.

The corresponding collective state has a spin of 1^- in even–even nuclei and is at a high excitation, perhaps 10–25 MeV above the ground state. It is known as the *giant* (*electric*) *dipole resonance* and is a prominent feature in many nuclear reactions, especially in the photodisintegration of both even- and odd-mass nuclei (Fig. 8.10). The dipole resonance can also be given a shell-model interpretation (Sect. 8.6.1) and the parity change shows that transitions between two major shells must be involved. The excitation energy as a function of A is about twice the value predicted for the shell spacing (eqn (7.3)) but the introduction of the proper residual interactions in a system containing both an excited particle and a hole is found to predict a collective dipole state that is pushed up in energy. The effect is similar, but opposite in sign, to the lowering of ground states by the pairing interaction discussed in Section 6.4.3.

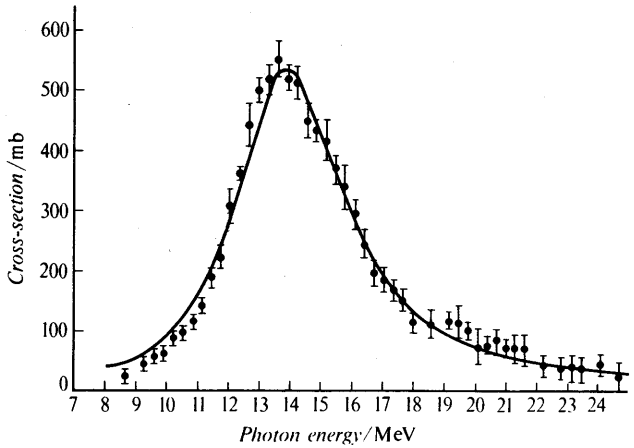

Fig. 8.10 Giant resonance of photodisintegration in ^{197}Au. The yield of neutrons is shown as a function of the energy of the monochromatic photons used to produce the reaction (Fultz, S. C. *et al.*, *Phys. Rev.*, **127**, 1273, 1963).

(iii) $\lambda = 2$ (Fig. 8.9*c*). Among the lowest-lying states, quadrupole phonons describe the most important excitations since the $\lambda = 0$, 1 modes have the special features just discussed. In the shell-model picture quadrupole excitation does not require a parity change and may, therefore, take place *within* a major shell provided that it is not full, as in closed-shell nuclei. For even–even nuclei the excitation energies above the 0^+ ground state are

$$E(n_2) = n_2 \hbar \omega_2 \tag{8.27}$$

where n_2 is the number of quadrupole phonons and the total angular momentum permitted for a given n_2 is determined by the occupation numbers allowed by the Bose–Einstein statistics. The spin values for a few values of n_2 are shown in Table 8.1.

TABLE 8.1 States deriving from quadrupole phonons (from Ref. 8.1, p. 347)

n_2 \ Spin I	0	1	2	3	4	5	6	7	8
0	1								
1			1						
2	1		1		1				
3	1		1	1	1		1		
4	1		2		2	1	1		1

The systematic appearance of the 2^+ single phonon vibrational state is an outstanding feature of the spectra of even–even nuclei, and the triplet of 2-phonon states 0^+, 2^+, 4^+ at approximately double the energy of the first excited states is also frequently seen, though other states are often present in the same region; Figure 8.11 shows the low levels of ^{114}Cd, which illustrate the point; they lie within the energy gap in the spectrum of intrinsic states.

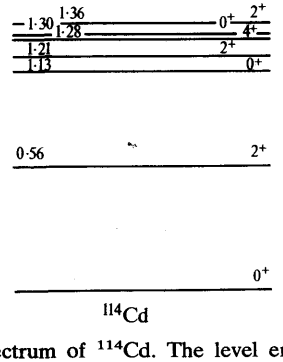

Fig. 8.11 Vibrational spectrum of ^{114}Cd. The level energies in MeV are shown together with spin-parity I^π.

Quadrupole modes of much higher energy, corresponding with particle excitations across two major shells, have also been seen and form a *giant quadrupole resonance* in the region of unbound levels near the giant dipole state. Evidence for this resonance is discussed in Reference 8.3.

(iv) $\lambda = 3$ (Fig. 8.9*d*). Octupole phonons have an energy approximately twice that of a quadrupole vibration, and the single-phonon octupole state (3^-) is found in the spectrum of even–even nuclei near the two-phonon quadrupole states. The collective 3^- excitation is a prominent feature among the low-lying states of these nuclei as revealed by inelastic scattering experiments.

(v) *Coupling of vibration with intrinsic motion.* For an intrinsic state with angular momentum $\boldsymbol{J}$ and a vibrational state with angular momentum $\boldsymbol{R}$, a multiplet of states arises with quantum number I given by

$$I = J+R, J+R-1, \ldots, |J-R| \tag{8.28}$$

For weak coupling between the two motions, in which the energy differences produced are small compared with the separation of intrinsic states and the two motions are independent, collective effects are due to the vibrational transition. A well-known example of this coupling is found in the spectrum of ^{209}Bi in which a 3^- octupole phonon, effectively an excitation of the ^{208}Pb core, is coupled to a $h_{9/2}$ single-proton state, yielding resultant I-values from $\frac{3}{2}$ to $\frac{15}{2}$.

Often the coupling between the two motions is strong, the pattern of excited states does not show such clear regularities, and the nucleus may acquire a stable deformation.

8.4.3 Energy levels (deformed equilibrium)

When the deformed nuclear shape becomes stable, in accordance with the potential-energy curve shown in Fig. 8.3*b*, vibrational modes may be based upon this equilibrium shape. The main types of vibration for a quadrupole deformation, for instance, may also be discussed in terms of phonons, but the order λ is not a good quantum number in a non-spherical field. The projection ν of the phonon angular momentum along the symmetry axis may be specified and two simple types of vibration, with $\nu = 0$ (β-vibration) and $\nu = \pm 2$ (γ-vibration), may be identified. These are illustrated in Fig. 8.12, which shows that β-vibrations preserve the axis of symmetry, while γ-vibrations do not.

Phonon numbers n_β and n_γ may be ascribed to the two types of vibration and, together with the K-value from any intrinsic motion, define the spin of the vibrational state. Rotational bands may be built upon each such state; the direction of rotation is indicated in Fig. 8.12.

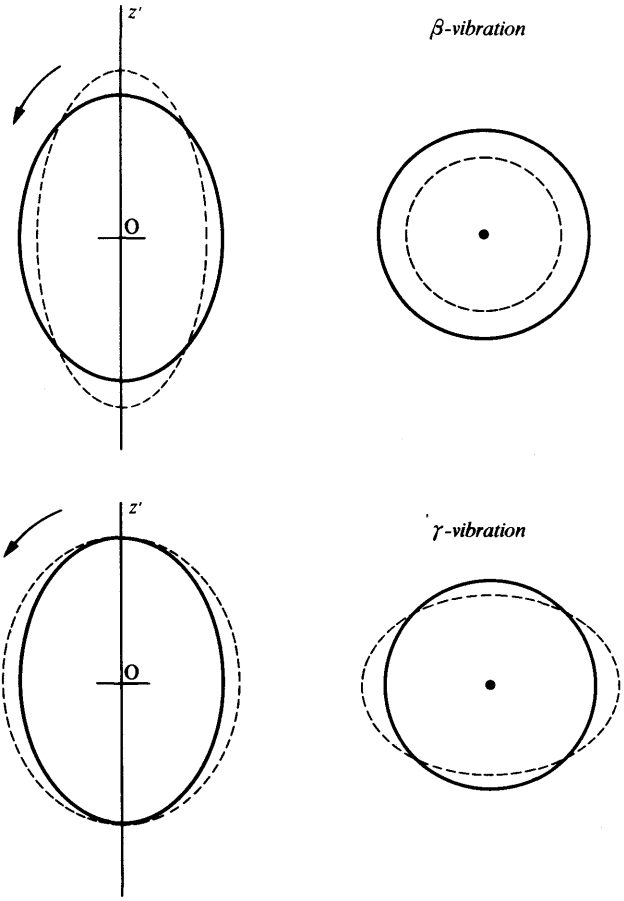

Fig. 8.12 β and γ vibrations of a distorted nucleus. The symmetry axis Oz' is shown and the diagrams at the right are sections in the equatorial plane. The full line is the equilibrium contour, the dotted line is one extreme excursion. The arrow shows the direction of rotation in a rotational band.

8.4.4 *Pairing vibrations; superfluidity*

The readiness with which like nucleons or nucleon holes form pairs with spin-parity 0^+ has frequently been referred to; it is the basis of the success of the single-particle shell model, and implies a strong correlation due to short-range attractive forces in the motion of the two particles. A pair may be regarded as a special form of collective excitation, resembling a vibrational quantum with $\lambda^\pi = 0^+$, $T = 1$ obeying Bose–Einstein statistics. A nucleus excited by one such quantum, e.g. a neutron pair, becomes the corresponding nucleus

with two extra neutrons and with the 'pair-vibrational' quantum energy.

Starting with a closed shell of neutrons, successive addition of such quanta produces a sequence of nuclei (e.g. $^{204}Pb \rightarrow {}^{206}Pb \rightarrow {}^{208}Pb$) with neutron numbers differing by 2 and with uniformly spaced ground state energies, if perturbations are neglected. This is analogous to the spectrum of a harmonic oscillator; in the present case the states may be labelled by the total isospin whereas for the oscillator the corresponding label is l, the angular momentum (Sect. 1.4.2). These states may be studied in two-particle transfer reactions of the type (t, p) or (p, t) (Sect. 11.5).

The ground state of a nucleus with many particles outside a closed shell contains a number of 0^+ pairs and is potentially in a superfluid condition as discussed for nuclear matter (Sect. 6.4.3). In a macroscopic superfluid such as HeII, correlations arise because of coupling between electronic motions and lattice vibrations and there is a coherence length of the order of atomic dimensions. In nuclei the 0^+ pairs can only be located within the nuclear dimension and the relative coherence is not so marked. The familiar properties of superfluid systems are, therefore, not clearly apparent in nuclear behaviour, except for the existence of the energy gap in the spectrum of intrinsic states in an even–even nucleus (Sect. 6.4.3).

8.5 Static and transition moments

The collective model was developed to explain the large static electric quadrupole moments observed, for example, in the rare-earth nuclei (Sect. 7.2.3). The quadrupole moment Q_0 in the body-fixed system is given by equation (3.32) and for a simple axially symmetrical deformation (Fig. 8.4) specified by the parameter δ we have, if the charge density is uniform (Ex. 8.3),

$$Q_0 = \tfrac{4}{5} Z R^2 \delta \tag{8.29}$$

where R is the equivalent spherical radius. The spectroscopically observed quadrupole moment is related to Q_0 by the expression

$$Q_I = \frac{3K^2 - I(I+1)}{(I+1)(2I+3)} \cdot Q_0 \tag{8.30}$$

for the state $K = I$, i.e.

$$Q_I = \frac{I(2I-1)}{(I+1)(2I+3)} \cdot Q_0 \tag{8.31}$$

where the ratio between Q_I and Q_0 is required because of averaging of the direction of the nuclear axis due to the rotational motion. For $I = 0$ and $I = \frac{1}{2}$, Q_I vanishes, although Q_0 may still exist. For very

large I, $Q_I \to Q_0$. The Q_0 values obtained in this way for the rare-earth nuclei are about 10 times the single particle value, which is of the order of R^2, and suggest δ-values of about 0·2, using (8.29). The states of a rotational band are connected by electric quadrupole radiation ($\Delta I = 2$) and the probability of this process depends on Q_0^2. The corresponding transition moments for deformed nuclei are very much larger than the single-particle values (Sect. 9.2) as illustrated in Fig. 8.13, and the values of δ obtained from transition rates agree with the evidence from static moments.

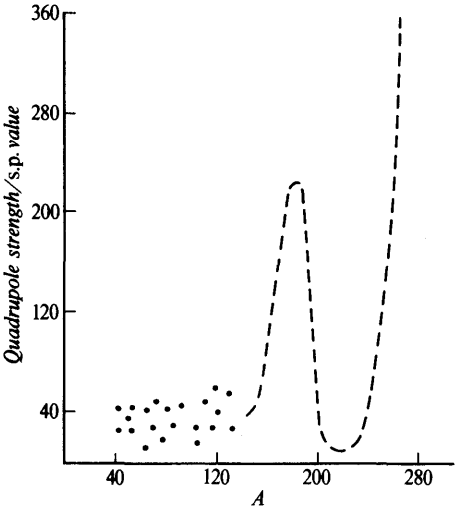

Fig. 8.13 Ground state electric quadrupole ($2^+ \leftrightarrow 0^+$) transition strength, in units of single-particle value, as a function of mass number A (adapted from Ref. 8.1).

Magnetic moments are also better predicted by the collective model than by the single-particle shell model. In a $K = 0$ rotational band there is no magnetic moment due to the intrinsic motion and

$$\mu_I = g_R I \mu_N \tag{8.32}$$

where g_R is the *rotational* g-factor. The magnetic moment is also a factor in the probability for magnetic dipole radiation but this cannot occur between the states of a rotational band with $K = 0$ because it requires $\Delta I = 1$. Measured g_R-factors are $\leqslant Z/A$, which is the classical value for a charged rigid body.

In rotational bands with $K \neq 0$ there is a contribution to the magnetic moment from the intrinsic motion, with a g-factor g_K. The static moment for $K > \frac{1}{2}$ is given in Reference 8.1 as

$$\mu_I = \left\{ g_R I + (g_K - g_R) \frac{K^2}{I+1} \right\} \mu_N \tag{8.33}$$

and the magnetic dipole transition probability includes a factor $(g_K - g_R)^2$. The factor g_K is smaller than the single particle or rigid body value, and the magnetic moments move off the Schmidt lines (Sect. 7.2.3) as required by observation.

8.6 The extended shell model

8.6.1 General approach

The energy of a nucleus containing A nucleons may be written as a sum of kinetic and potential energy terms, i.e.

$$\text{Total energy } H = \sum_{i=1}^{A} T_i + \sum_{i<j} V_{ij} \tag{8.34}$$

where V_{ij} is the mutual potential energy for nucleons i, j. The SPSM, described in Chapter 7, approximates this to the form

$$H_{SP} = \sum_{i=1}^{A} (T_i + U_i) + \sum_{i<j} v_{ij} \tag{8.35}$$

where $T_i + U_i$ is now the total energy of a single nucleon obtained by solving the wave equation for a nucleon moving independently in a central field in which the one-body potential energy is U_i. The residual interactions v_{ij} are neglected except for the assumption that nucleons outside closed shells pair off as far as possible with antiparallel spins and orbital momenta. The model has been surprisingly successful in predicting the level sequences for many odd-mass nuclei, and especially for those with nucleon numbers near major closed shells, e.g. $^{209}_{82}$Pb, but, as noted in Chapter 7, it fails to predict many observed nuclear moments. Moreover, it cannot account for the fragmentation of the single-particle levels observed in nuclei with several 'valence' particles outside the shells. Extension of the model involves consideration of both its major assumptions, namely the independence of motion in a central potential, and the incomplete treatment of the residual interactions.

It has been seen in Section 6.4 that an average field, which essentially creates the one-body shell model potential, is a property of nuclear matter; it will, therefore, plausibly be a property of finite nuclei. For a nucleus it might therefore be thought that the ground state wavefunction could be obtained by a calculation of the *Hartree–Fock* type that has been so successful for atoms. In such calculations the central field is made *self-consistent* by allowing the wavefunctions that it predicts to modify the field itself in which the particles move. A variational procedure then determines both the potential and the wavefunctions that give a minimum energy. Unfortunately, this procedure will not work so simply for nuclei, because of the existence of the repulsive core in the internucleon

force (potential V_{ij}, eqn (8.34)). It is necessary, in fact, to use the methods developed for nuclear matter calculations and in particular the Brueckner effective potential or G-matrix (Sect. 6.4). The calculations are complex and difficult but they have been made for the double-closed-shell nuclei ^{16}O, ^{40}Ca and ^{208}Pb and may be used to check the validity of more approximate calculations in which simplifying assumptions are made.

In many such calculations the single-particle energies $(T_i + U_i)$ of equation (8.35), in which kinetic energies appear, are taken directly from experimental data. Attention is then concentrated on the potential energy shifts due to the residual interaction v_{ij}, and on the single-particle states that may be occupied by the particles between which the residual forces act; these states define the *model space* of the IPM (independent-particle model) introduced at the beginning of this chapter. Levels in this model are specified by the symbols (I^π, T) where π denotes the parity. The procedure for calculating a level spectrum is to specify the nucleon configuration that may contribute to the wavefunction of a given level and then to evaluate the matrix elements of the assumed residual interaction between the states of the model space. These matrix elements are to be understood in terms of collisions between two interacting particles (see Fig. 8.14*b*) in which there may be an exchange of orbital motion although angular momentum $\boldsymbol{j}$ is conserved overall. Finally, using these matrix elements augmented by single-particle terms and spin-orbit energies the full Hamiltonian matrix is set up. From this the eigenvalues giving the energies of the states and the eigenvectors giving their wavefunctions are obtained by standard methods. The eigenfunctions can then be used in the evaluation of nuclear moments and transition probabilities.

The calculation of the matrix elements should ideally employ self-consistent wavefunctions, but oscillator functions are generally used for convenience, with an extent chosen to match the nuclear radius. Their use has been justified in some cases by comparison with the results of a Hartree–Fock calculation. The residual interaction v_{ij} should be consistent with what is known of the two-body force (Sect. 5.8) in nuclear matter (Sect. 6.4), but the general trend of level energies can be shown by using rather simple forms of force. In the early work of Edmonds and Flowers and of Elliott and Flowers, particularly for p-shell nuclei, Yukawa or Gaussian forces were used with a specific set of exchange operators and the energy-level spectrum was studied as a function of the range of the force and of the angular momentum coupling scheme (*LS* or *jj*). An even simpler force is the *surface-delta* interaction, which exists only in the nuclear periphery and for identical coordinates of the interacting particles. An example of the use of this interaction will be given in the next section.

More realistic calculations must introduce the repulsive core of the internucleon force and a method of doing this was developed by Kuo and Brown (Ref. 8.2) using the techniques of the nuclear matter problem, but confining attention still to only a small number of configurations. When the residual interaction is set up in this way, so that the resulting Hamiltonian acting on a limited range of wavefunctions produces a result hoped to be equivalent to those of a full, unlimited calculation, it is said to be an *effective interaction.* Calculations using effective interactions and experimental single-particle energies can now be made on a very large scale, using several nucleons distributed between several single-particle levels. Such work, in fact, predicts some levels which would normally be thought to form a band, and this emphasizes the basic connection between shell-model states and nuclear deformations.

Finally, it may be noted that in the work of Kuo and Brown, allowance was made for levels resulting from the one-particle, one-hole (1p–1h) configuration in which a nucleon is elevated from the core to a valence state. In light nuclei at least such excitations may form both the 1^- ($T=1$) giant dipole state and the 3^- ($T=0$) octupole state, which were previously given a collective interpretation. The observed energies of these states can be understood in this shell-model picture by introducing the particle–hole interaction, which is attractive in $T=0$ states and repulsive in states of $T=1$. Intervention of such core excitations also seems necessary in order to remove remaining discrepancies in predicted electromagnetic transition probabilities.

8.6.2 *Typical calculation – the nucleus* ^{18}O

The low-lying energy levels of the nucleus ^{18}O are shown, together with their spins and parities, in Fig. 8.14*a*. From the neutron and proton numbers $N=10$, $Z=8$ the isobaric spin component is $T_z=-1$, so that the isobaric spin T itself must be at least 1 for all levels. Since the lowest levels have analogue states in just two other nuclei (^{18}F, ^{18}Ne) we conclude that these levels have $T=1$.

The SPSM suggests that for an inert ^{16}O core ($Z=N=8$, $I^\pi=0^+$) the two extra neutrons may occupy the 2s or 1d levels or both. Possible configurations for a state $(I, T)=(0, 1)$ with jj-coupling would be

$$(1d_{5/2}^2; 0, 1), \qquad (2s_{1/2}^2; 0, 1), \qquad (1d_{3/2}^2; 0, 1) \tag{8.36}$$

in an obvious notation and for the state (2, 1) the first and last of these are also possible together with

$$(1d_{5/2}2s_{1/2}; 2, 1), \qquad (1d_{5/2}1d_{3/2}; 2, 1), \qquad (1d_{3/2}1s_{1/2}; 2, 1) \tag{8.37}$$

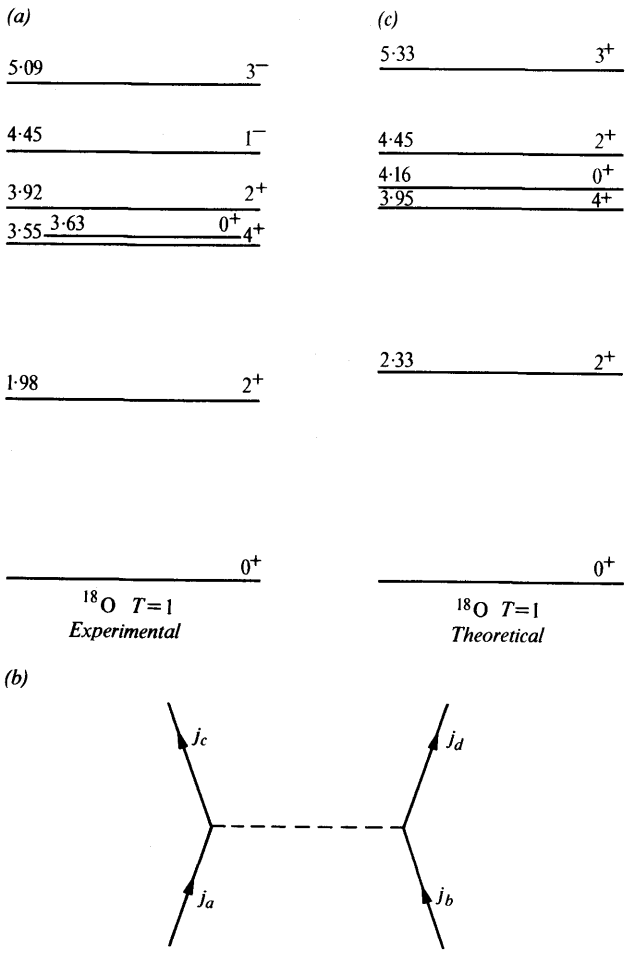

Fig. 8.14 (*a*) Low-lying levels of ^{18}O (experimental). (*b*) Interaction between two nucleons in a bound state, $\boldsymbol{j}_a + \boldsymbol{j}_b = \boldsymbol{j}_c + \boldsymbol{j}_d$. (*c*) Even-parity ^{18}O levels predicted by T. T. S. Kuo and G. E. Brown (Ref. 8.2) allowing for core excitation.

making five in all for this state. All the states (8.36) and (8.37) are symmetrical for exchange in isospin because they relate to two identical particles and they are of even parity because only the angular momenta $l = 0, 2$ are involved. Levels (3, 1) and (4, 1) can also be formed from some of these configurations.

The space wavefunctions ϕ of the two nucleons are usually taken to be eigenfunctions $R_{nl}Y_l^m$ of the oscillator potential. The two-nucleon wavefunction is then constructed, in analogy with similar constructions in the theory of the helium atom, using the standard

coupling procedure for angular momenta described in Appendix 4. It is an eigenfunction of the total angular momentum operator and has the form

$$\psi(j_1 j_2; IM) = \sum_{m_1} (j_1 j_2 m_1 m_2 \mid IM)\phi_1(j_1 m_1)\phi_2(j_2 m_2) \qquad (8.38)$$

where j_1, j_2 are the individual angular momenta and m_1, m_2 $(=M-m_1)$ their resolved parts, coupling to the two-particle state of spin I and resolved part M. If $j_1 \neq j_2$ (8.38) should be antisymmetrized, but for $j_1 = j_2$ it is, in fact antisymmetric for even values of I (see Ex. 8.10). Since only $T=1$ states are involved the isobaric spin coupling coefficient $(\frac{11}{22} -\frac{1}{2} -\frac{1}{2} \mid 1\ -1)$ is unity. Each individual j is composed of a spin part and an orbital part, and the component wavefunctions may be expressed

$$\phi_1(j_1 m_1) = \sum_{m_l m_s} (l_1 s_1 m_l m_s \mid j_1 m_1)\phi_L(l m_l)\phi_S(s m_s) \qquad (8.39)$$

The wavefunction for a given state of ^{18}O is a linear combination of the two-particle states (8.38) which form a model space in this example.

For the surface-delta interaction a specific formula for the matrix elements $\langle j_a j_b \mid v \mid j_c j_d \rangle$ of the residual interaction v is given by Glaudemans *et al.* (*Nuclear Physics* **A102**, 593 (1967)), together with an empirical value of the interaction strength. Matrices can, therefore, be set up for the 0^+, 2^+, 3^+ and 4^+ states (see Ex. 8.11). Each matrix element is adjusted for the spin-orbit energy, which is known empirically from the $d_{5/2}$–$d_{3/2}$ doublet separation in ^{17}O. One of the states, e.g. 4^+, is then made to have its observed energy and this gives a further term to be added to the diagonal matrix elements; this is the same for all states if the 2s and 1d nucleons are described by a harmonic oscillator potential (in which these two states are degenerate) and if the effect of the ^{16}O core is the same in all states. The energies of the remaining states 0^+, 2^+, 3^+ then follow as solutions of the eigenvalue problem. Orthogonal states of the same spin-parity but at higher energy are also found in the calculation.

Example 8.11 gives numerical results for an even further simplified calculation for ^{18}O, excluding the $d_{3/2}$ states and the 3^+ level. The more realistic predictions given by Kuo and Brown are shown in Fig. 8.14*c*. These reproduce the lowering of the 0^+ ground state that is an example of the energy gap well known in fermion systems. The 2^+ state is also lowered for similar reasons.

8.7 Study of the nuclear level spectrum

Experimentally, level sequences and properties may indicate the nature of the nuclear Hamiltonian, revealing the presence or absence of collective or single-particle effects. By far the greatest

amount of information on these properties, for comparison with the theories outlined in this and the preceding chapter, is obtained from nuclear reaction experiments. Such dynamical processes have an interest of their own, particularly in the processes of fission and fusion, and they will be described in the following chapters with some emphasis on the information that they offer on nuclear levels. The processes chiefly used are summarized below for particular properties.

(i) *Wavefunction.* Static moments of levels (Sect. 3.4) and radiative transition probabilities between them (Sect. 9.2) are obtained directly from wavefunctions by the application of suitable operators. In nuclear reactions the spectroscopic factor (Sect. 11.5.2) measures the extent to which a wavefunction represents that of a single-particle level.

(ii) *Excitation energy.* Discrete levels are studied by nuclear reactions such as deuteron stripping or pickup. Such transfer reactions strongly excite single particle or hole levels, whereas inelastic scattering preferentially excites collective modes. Low-lying levels are excited by α- and β-decay of radioactive parents.

(iii) *Width or lifetime.* The (radiative) width of bound levels is generally so small that direct measurement is impossible except under the special circumstances offered by the Mössbauer effect (Sect. 9.4.4). The widths Γ are obtained from lifetime measurements (see eqn (9.11) and Sect. 9.4) or from the cross-section for Coulomb excitation (Sect. 9.4.2).

Virtual levels have particle widths as well as radiative widths and may be determined from the shape of resonance or transmission curves.

(iv) *Spin, parity and isospin.* Information on these quantum numbers comes from angular distribution experiments, both for production and decay of the states, and from the operation of selection rules in these processes. Identification of isobaric analogue states in a range of nuclei may fix the total isospin number T.

In discussing these processes in the following chapters it will be convenient to group them under the headings of the three main interactions, electromagnetic, weak and strong, though it will rapidly become clear that rigid boundaries cannot be drawn.

8.8 Summary and survey of nuclear spectra

Collective and independent-particle modes of motion in nuclei are superficially distinct and each describes a special group of experimental facts. More fundamentally, however, these two models must be unified, and there is evidence from Hartree–Fock calculations that this is possible. An intermediate step is the Nilsson model in

which shell-model orbits are set up in a deformed potential that is chosen semi-empirically.

From a phenomenological point of view, it is apparent that the most important parameter for an understanding of the general nature of the low-lying (bound) levels is the number of particles outside a closed shell or the number needed to complete a shell. Figure 8.15 illustrates the change in the pattern of observed levels as the number of holes increases from the doubly-magic nucleus $^{208}_{82}$Pb. In ^{207}Pb the intrinsic single-particle (i.e. hole) levels of the spherical potential are found, in ^{206}Pb there is a two-hole spectrum showing the depression of the 0^+ ground state and 2^+ excited state with respect to the higher levels as a result of coherence associated with the pairing interaction.

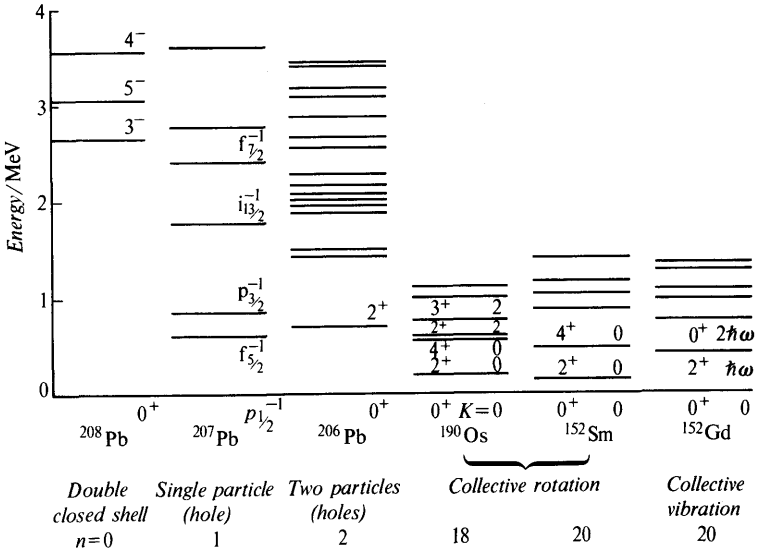

Fig. 8.15 Sketch of level spectra with increasing number (n) of particles outside, or holes in, a double-closed shell.

From ^{190}Os to ^{152}Sm, the even–even nuclei show the rotational spectra of the deformed shape, while at ^{152}Gd the deformation is small and the vibrational spectrum of the spherical shape is seen. When allowance is made for the $A^{-1/3}$ dependence of level spacings (eqn (7.3)), it is found that the lower rotational and vibrational states lie within the energy gap in the intrinsic states of an even–even nucleus.

At excitation energies well above the nucleon binding energy, the most prominent features of nuclear spectra are the giant states, which are envelopes of several MeV width corresponding with excitations that traverse one or two major shells. In the same region

of virtual levels, the isobaric analogue states of ≈100 keV width (Sect. 5.6.1) are located. Figure 8.16*a*, taken from Reference 8.3a, relates the giant resonance states to the bound levels and to the so-called 'statistical' region of levels (Sect. 11.3) in which the concept of a level spectrum loses its meaning. Figure 8.16*b* is an energy-level schematic conveying similar information.

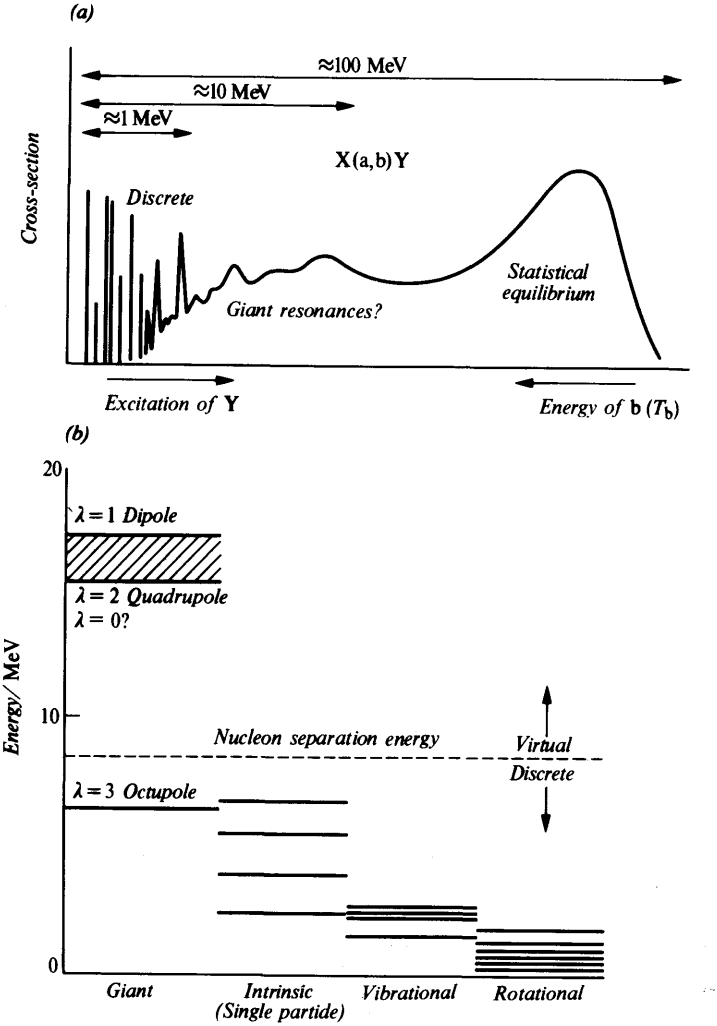

Fig. 8.16 (*a*) The nuclear level spectrum, as seen in the energies of particles b emerging from a nuclear reaction X(a, b)Y* with bombarding energy ≈100 MeV. The energy scale gives both the energy T_b and the resulting excitation of the nucleus Y (Ref. 8.3*a*). (*b*) Schematic of main features of a nuclear level spectrum, showing different types of state.

Examples 8

8.1 Find the excitation of the compound nucleus ^{108}Ag in process (8.3) if it is produced by the absorption of a neutron of energy 1 eV. Assume that the values of $M-A$ in keV for the nuclei concerned are n, 8072; ^{107}Ag, −88 408; ^{108}Ag, −87 605. What precision in the measurement of $(M-A)$ would justify the inclusion of a correction for the neutron energy? [7269 keV]

8.2 Consider two masses M bound together with an equilibrium separation R. Estimate the order of magnitude of the lowest rotational frequency of the system, and compare it with the vibrational frequency due to a vibrational amplitude βR. [$\omega_v/\omega_r \approx 1/\beta^2$]

8.3* Calculate the intrinsic quadrupole moment of a uniformly charged ellipsoidal nucleus with major and minor semi-axes a, b.

If the deformation parameter δ is defined by the equation

$$\delta = \tfrac{3}{2}(a^2-b^2)/(a^2+2b^2)$$

show that the quadrupole moment of a nucleus with Z protons located at points r_k may be written

$$Q_0 = \frac{4}{3}\left\langle \sum_{k=1}^{Z} r_k^2 \right\rangle \delta$$

By finding $\langle \sum r_k^2 \rangle$ for a spherical distribution of sharp radius R show also that

$$Q_0 = \tfrac{4}{5} Z R^2 \delta$$

8.4 A rotational band based on the state $K=\frac{7}{2}^-$ is known in $^{179}_{74}$W. The $\frac{9}{2}^-$ state is at an excitation of 120 keV; predict the excitations of the $\frac{11}{2}^-$, $\frac{13}{2}^-$ and $\frac{15}{2}^-$ levels. [267, 440, 640 keV]

8.5* The nucleus $^{234}_{92}$U has levels of spin-parity 0^+, 2^+, 4^+, 6^+, 8^+ at energies of 0, 44, 143, 296 and 500 keV. Show that these form a rotational band, predict the energy of the 10^+ state, and check the variation of the moment of inertia of the nucleus with rotational frequency. Compare the moment of inertia with the rigid-body value.

8.6* Prove equations (8.15) and (8.16).

8.7 Using equations (8.15) and (8.16) study the variation of moment of inertia with rotational frequency for the ground state band of ^{158}Er using the following energies for the successive electric quadrupole transitions upwards through the band from $I=2\rightarrow 0$ to $I=16\rightarrow 14$: 192·7, 335·7, 443·8, 523·8, 578·9, 608·1, 510·0, 473·2 keV. (Ward, D. *et al. Phys. Rev. Lett.* **30,** 493, 1973)

8.8 Using equation (8.18) and the information on ^{169}Tm in Fig. 8.6c, estimate the decoupling parameter a. [−0·78]

8.9* Write down the μ-values for two quadrupole phonons and verify that the states which are symmetrical under exchange have the angular momenta shown in Table 8.1 for $n_2=2$.

8.10* Show that for two nucleons in the same j-shell, the $T=0$ states have I odd and the $T=1$ states have I even.

[Express the angular momentum wavefunction in terms of single-particle functions as in equation (8.38) and consider the effect of nucleon exchange. Use the Clebsch–Gordan property

$$(j_1 j_2 m_1 m_2 \mid IM) = (-1)^{j_1+j_2-I}(j_1 j_2 m_2 m_1 \mid IM)]$$

For the case of two $p_{3/2}$-protons, write out the m_l and m_s values explicitly and verify the grouping into states of $I=0$ and $I=2$.

8.11* Calculate the spacing of the 0^+ and 2^+ levels of the nucleus ^{18}O relative to the 4^+ level due to an effective interaction in the $d_{5/2}$ and $s_{1/2}$ states only (i.e. omitting $d_{3/2}$ and the 3^+ level). Take the energy of the 4^+ state to $-0{\cdot}35$ MeV, the $(d_{5/2}$–$d_{3/2})$ doublet splitting in ^{17}O to be $5{\cdot}08$ MeV, and use the following matrix elements of Kuo and Brown (in MeV) for the residual interaction:

	$\langle \frac{5}{2}\frac{5}{2}\|v\|\frac{5}{2}\frac{5}{2}\rangle$	$\langle \frac{5}{2}\frac{5}{2}\|v\|\frac{5}{2}\frac{1}{2}\rangle$	$\langle \frac{5}{2}\frac{1}{2}\|v\|\frac{5}{2}\frac{1}{2}\rangle$
$I=4^+$	0·14		
$I=2^+$	−0·94	−0·81	−1·09
$I=0$	−2·53	−1·09	−2·35

Find the corresponding eigenfunctions.